JOURNAL OF VIROLOGY, Feb. 1978, p. 596-607
0022-538X/78/0025-0596$02.00/0

Vol. 25, No. 2
Printed in U.S.A.

Biological Properties and Physical Map of the Genome of a New Papovavirus, HD Virus

KLAUS BOSSLET AND GERHARD SAUER*

Institut für Virusforschung, Deutsches Krebsforschungszentrum, 6900 Heidelberg, West Germany

Received for publication 25 August 1977

The superhelical DNA of the HD papovavirus is heterogeneous and consists of two discrete size classes with molecular weights of 3.45×10^6 and 3.25×10^6. Both size classes of DNA are encapsidated into HD virion particles. Their relative intracellular amounts differ, depending on the cell system. Vero-76 carrier cultures in which HD virus was detected contain both size classes of DNA, with the larger molecules prevailing by a factor of 10. Five clonal lines derived from Vero-76 cell cultures contain exclusively the larger DNA. On the other hand, after cocultivation of Vero-76 with CV-1 cells for several passages, minicircular DNA is accumulated such that both size classes are synthesized in equal amounts. Any of the originally viral DNA-producing cell lines may, upon subcultivation, cease yielding virus. The RITA cell line of *Cercopithecus aethiops* origin is the only cell line among numerous ones tested which upon infection permits the establishment of a one-step growth cycle. However, between 6 and 8 days after infection, viral DNA synthesis is discontinued, and a persistent viral infection cannot be established. Physical maps of the genomes were constructed, and it could be shown that the smaller, minicircular DNA had originated from the larger DNA as the result of a deletion. The sequences missing in the minicircular DNA are confined to the relative map position 0.15 to 0.21.

A new transforming papovavirus, designated HD virus, was isolated recently in our laboratory from Vero cells (9). The Vero cell line, which originated from a monkey kidney (*Cercopithecus aethiops*), was established in 1963 (10) and since then has been widely distributed to numerous laboratories. Although we have examined Vero cells from various sources, we have been unable to demonstrate the presence of either HD virus or HD superhelical DNA in any of the cell cultures, except within the Vero line, which has been grown for more than 5 years in our laboratory. The virus multiplies without cytopathic effect in our Vero cells. It does not grow in closely related cells of *C. aethiops* origin, such as CV-1 and other Vero cultures, or in some cultures of human origin. The only permissive host cell system so far available is RITA cells, which are derived from the same species. In these cells, HD virus DNA replicates, although only to a limited extent.

As we have shown recently, the size and structure of HD virus resemble those of simian virus 40 (SV40) virions, and it is ether resistant, contains superhelical DNA, and is capable of transforming Vero cells in vitro. It is interesting to note that in DNA-DNA hybridization experiments, HD virus proved to be unrelated to the other members of the SV40-polyoma subgroup, which all share some common base sequence homology with each other (9). Also, anti-SV40 tumor antigen and capsid antisera do not cross-react with HD virus-infected cells.

In this study the growth kinetics and the DNA of HD virus are discussed. It is shown that there exist two discrete size classes of HD superhelical DNA, one of which is deleted within a defined region. It is unusual that the relative amounts of the two superhelical forms can be altered depending on the host cell system used for propagation. Physical maps of both the larger and the deleted HD virus genomes are presented.

MATERIALS AND METHODS

Cells. Vero cells were grown in Eagle minimum essential medium supplemented with 10% calf serum. Clonal lines (designated Vero-clones A to E) were established from our HD virus-containing Vero cells (designated Vero-76) by isolating colonies that were formed in soft agar (6). Cocultivation of Vero-76 cells with CV-1 cells (4) was performed by mixing equal numbers of cells from both lines, which were then passaged together. RITA cells (Italdiagnostic, Rome), 3T3, Wi38, BSC-1, and HeLa cells were grown in a similar manner to Vero cells in Eagle minimum essential medium supplemented with 10% calf serum. The LLC-macacus rhesus cell line was kindly provided by the Ehrlich Institut, Frankfurt.

Virus. HD virus was harvested from Vero-76 cells,

Vero-clone E, which proved to be the best virus yielder among the different clones, or cocultivated Vero-76–CV-1 cell cultures. The virus was liberated from the cells (10^7 or more cells grown in large roller vessels) by two cycles of freezing and thawing, as described previously (9). Then the cellular debris was removed by low-speed centrifugation in a Christ-Heraeus Minifuge (4,000 rpm, 10 min). The supernatant (adjusted to 10 mM $MgCl_2$) was digested with pancreatic DNase (100 μg/ml) for 60 min at 37°C and shaken for 5 min, with an equal volume of ether to inactivate putative RNA tumor viruses that might be present as contaminants. After removal of the ether by bubbling N_2 through the solution and sterile filtration through a Millex filter (pore diameter, 0.22 nm; Millipore Corp.), the virus-containing fluid was used for infection.

Virus purification. The virus-containing fluid, prepared as described above, was adjusted to a final concentration of 0.5 M NaCl and 10% polyethyleneglycol. After 18 h at 4°C, the suspension was centrifuged in a Christ-Heraeus centrifuge for 15 min at 4,000 rpm. The pellet was suspended in 2 ml of 20 mM Tris (pH 7.5) and dialyzed for 1 day against 3,000× the volume of the same buffer. The virus was further purified by equilibrium density gradient centrifugation in CsCl (adjusted to a refraction index of 1.3690 in 20 mM Tris, pH 7.5). One-half milliliter of the dialyzed virus-containing suspension was layered on top of the CsCl gradients and centrifuged for 3 days at 4°C and 38,000 rpm in a Spinco 50Ti rotor.

Preparation of labeled viral DNA. For radioactive labeling of HD viral DNA, the Vero cell cultures were incubated for between 4 and 6 days after seeding with 6 μCi (21 Ci/mmol) of [^{3}H]thymidine or 50 μCi of [^{32}P]orthophosphate per ml in phosphate-free medium. Selective isolation of the superhelical DNA and further purification of the DNA in CsCl-ethidium bromide (EtBr) density equilibrium gradients were as described for SV40 DNA (8). The fd DNA was a gift from H. Schaller, Institute for Microbiology, University of Heidelberg.

Slab gel electrophoresis. Electrophoresis was performed either in 1% agarose or 4% acrylamide vertical gels (sizes up to 60 by 20 by 0.3 cm) as described (3). The gels were stained after electrophoresis with EtBr (0.5 μg/ml) for 30 min and photographed using UV light. The distribution of radioactivity after electrophoresis was determined by cutting the frozen gels with a set of razor blades (distance, 1.1 mm) as described (8). Densitometer tracings of the stained gels were performed as described (2).

Preparative isolation of DNA from agarose gels. For separation of minicircular HD DNA from the larger HD DNA, between 50 and 100 μg of superhelical HD DNA was applied to 1.0% agarose gels (60 by 20 by 0.3 cm) and subjected to electrophoresis for 3 days at 4°C and 100 V. Under UV light the desired gel sections were excised and transferred into a glass homogenizer. After addition of 5 ml of 20 mM Tris–1 mM EDTA (pH 7.5), the agarose was homogenized (10 strokes). After incubation for 18 h at 4°C, the agarose was pelleted in a Christ-Heraeus Zeta 20 centrifuge for 20 min at 15,000 rpm. The DNA in the supernatant was adsorbed to a DEAE-cellulose column (bed volume, 2 ml) and eluted with 200 μl of triethylaminecarbonate. The eluate was desalted on Sephadex G50, lyophylized, and resuspended in 5 mM Tris–0.25 mM EDTA (pH 7.5).

Restriction endonuclease cleavage. Cleavage of HD DNA with endo R · *Hin*dII + III and endo R · *Eco*RI restriction endonucleases was performed as described (8). The DNA was treated with S_1 nuclease as previously described (8).

Blotting. Blotting and hybridization were performed as described (5). As radioactive probes, nick-translated minicircular HD DNA and CV-1 DNA were used after labeling with α-^{32}P-nucleotides (1).

RESULTS

Permissive conditions for the replication of HD DNA. The narrow host range of HD virus is confined as previously described (9) to the Vero-76 carrier cell cultures grown in our laboratory and to a related cell line, called RITA, which is also of *C. aethiops* origin. The virus is indigenous to the Vero-76 cells, whereas the RITA monkey kidney cell line has so far been found to be the only cell system in which a one-step growth cycle with HD virus could be accomplished. Infection is performed with lysates of virus producing Vero-76 cells (9), as described in Materials and Methods. Attempts to grow the virus on Wi38, human embryonic lung, HeLa, 3T3, and bovine cells have failed (9). Attempts to grow HD virus in Vero cells from various other sources, which were proven to be HD virus-free, were equally unsuccessful. It did grow in LLC cells of macacus rhesus origin, although close to the level of detectability and without producing a cytopathic effect. A further peculiarity of the HD virus is its failure to grow in CV-1 and BSC-1 cells, which are both closely related to RITA cells. The lack of a cytopathic effect precludes plaque assays for titration. Thus, as already described, the synthesis of superhelical HD FO I DNA after infection with Vero-76 cell lysates serves as a measure for infectivity (9). Furthermore, we have also previously shown that its growth closely depends on the physiological state of the host cells. To reveal both viral progeny and viral FO I DNA, it is essential that the cells (both Vero-76 carrier cultures and infected RITA cells) undergo active growth. In stationary cultures virus replication is almost completely curtailed (G. Sauer, W. Waldeck, and K. Bosslet, *Mosbacher Colloquium*, in press).

To establish one-step growth kinetics, RITA cells were used 1 day after seeding at a 1:3 split ratio, which ensures semiconfluency of the cells and permits mitotic activity over a period of at least 7 days (deduced from growth curves of RITA cells not shown here). Parallel cultures were infected with Vero-76 lysates, as described (9), and pulse-labeled with [^{3}H]thymidine for a

period of 2 days immediately after infection and between 2 to 4, 4 to 6, and 6 to 8 days after infection, respectively. After the labeling periods the DNA was isolated from the cell cultures and centrifuged into dye-buoyant density gradients to separate the superhelical HD FO I DNA from the cellular DNA. The relative amount of radioactive label in the position of the dense superhelix band indicates that the period of active HD FO I DNA replication lies between 4 and 6 days after infection (Fig. 1). Thereafter the viral DNA ceases to replicate. Compared to that of SV40, the growth cycle of HD is, therefore, considerably slower.

The yield of HD FO I DNA is also rather small and, apart from the fact that only logarithmically growing cell cultures are used for isolation of DNA, also depends on the passage level of the respective cultures (Table 1). As a standard system for HD FO I DNA production, Vero-76 cells are used that reveal, on average, 1.5 μg of DNA per 10^7 cells. Clones derived from Vero-76, such as clone E, proved to be as efficient as the uncloned culture with regard to HD DNA synthesis, but upon further passaging they completely lost their ability to yield viral DNA. This loss was paralleled, on the other hand, by a gain of growth potential and by a phenotypical change of the cells. If the cells had a fuzzy shape at the time of optimal viral DNA production, this appearance changed with increasing passage levels to a more "healthy" look and the cultures grew much faster. This alteration might be explained by a gradual loss of poorly growing, virus-yielding cells from the cultures, which might have been outgrown by more rapidly dividing non-virus yielders. A similar phenomenon was noticed when Vero-76 cells were cocultivated with CV-1 cells. Here, too, after an initial stimulation, a final drop in HD DNA synthesis occurred after several passages. We have not been able to establish a persistent infection in RITA cells, since after an initial viral DNA production this ability was lost upon five further passages of the cultures. Attempts to adapt HD virus by serial passages have also failed. For this purpose, RITA cells were infected with Vero-76 lysate. Six days after infection, the RITA cells were lysed and the total lysate was used for infection of a new RITA culture. This procedure was repeated five times, and then the cells were examined for the presence of HD FO I DNA. There was no discernible HD DNA (Table 1).

Two size classes of HD FO I DNA are encapsidated. Analysis of the superhelical HD

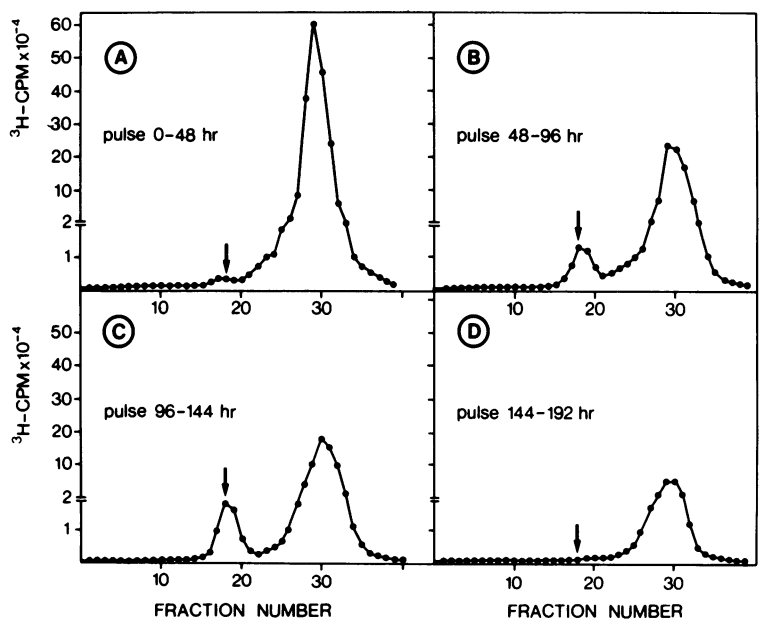

FIG. 1. *Growth kinetics of HD virus in RITA cells. Subconfluent parallel cultures of RITA cells (10^7 cells per flask) were infected with 10 ml of Vero-76 lysate as described (9) and labeled with [^{3}H]thymidine for various lengths of time. The selectively isolated DNA was quantitatively centrifuged into equilibrium in CsCl-EtBr density gradients, the profiles of which are shown here. The arrows indicate the position of SV40 FO I DNA in a separate gradient. (A) DNA labeled between 0 and 48 h; (B) DNA labeled between 48 and 96 h; (C) DNA labeled between 96 and 144 h; (D) DNA labeled between 144 and 192 h.*

FO I DNA preparations in agarose gels reveals the presence of two discrete size classes of molecules (Fig. 2). There is, in addition to the larger HD DNA, a smaller, minicircular FO I DNA class. The comparison with SV40 DNA shows that both DNA classes are smaller. Their relative amounts are subject to changes depending on the host cell system used for propagation. For example, Vero-76 clones A to E produce the larger form exclusively, whereas uncloned Vero-76 cells reveal both the larger and the minicircular DNA, with the larger size class prevailing by a factor of 10. The molar ratio can be changed for reasons that are not clear when Vero-76 cells are cocultivated with CV-1 cells (Fig. 2, gel A). In such a case an accumulation of minicircular DNA occurs to the extent that now both size classes are synthesized in equal amounts (as determined from densitometer tracings of the stained gels [not shown]). Synthesis of minicircular DNA in the absence of the larger molecules has not been found, with the exception of Vero-76 cells at earlier passage levels (9), where we cannot exclude, however, the presence of trace amounts of the larger class of FO I DNA.

The question arises as to whether both forms of DNA are being encapsidated into virion particles. Therefore, Vero-76 cells were incubated with [^{3}H]thymidine, and HD virus was purified as described in Materials and Methods. The virus suspension was mixed with ^{32}P-labeled, purified SV40 virions and centrifuged to equilibrium in a CsCl density gradient. It may be seen from Fig. 3 that HD virions band similarly to SV40 virions at a density of 1.337 g of CsCl per cm^3, with a shoulder towards the less-dense part of the gradient. When the virion DNA was pur-

TABLE 1. *HD FO I DNA production in various permissive cell systems*

Cell system[a]	Passage level	μg of DNA/5 × 10^7 cells[b]
Vero-76		1.5
Vero-76, clone A		0.35
Vero-76, clone E	10	1
Vero-76, clone E	25	0
Vero-76–CV-1	Cocultivated (passage 5)	2.5
Vero-76–CV-1	(passage 13)	0.01
RITA, HD infected[c]		1
RITA, HD infected[d]	5	0
RITA, HD infected[e]	5	0

[a] Subconfluent cell cultures were used for isolation of DNA 1 day after seeding.

[b] The data represent average values obtained from several experiments.

[c] Subconfluent RITA cells were infected with a VERO-76 lysate, and the DNA was extracted 6 days after infection.

[d] Subconfluent RITA cells were infected with a Vero-76 lysate, and 6 days after infection the RITA cells were lysed by freezing and thawing. The entire cell lysate was used for reinfection of a new subconfluent RITA cell culture. The same protocol was repeated five times. The DNA was then isolated.

[e] Subconfluent RITA cells were infected with a Vero-76 lysate, and the culture was passaged without further infection at 6-day intervals at a 1:4 split ratio five times before the DNA was isolated.

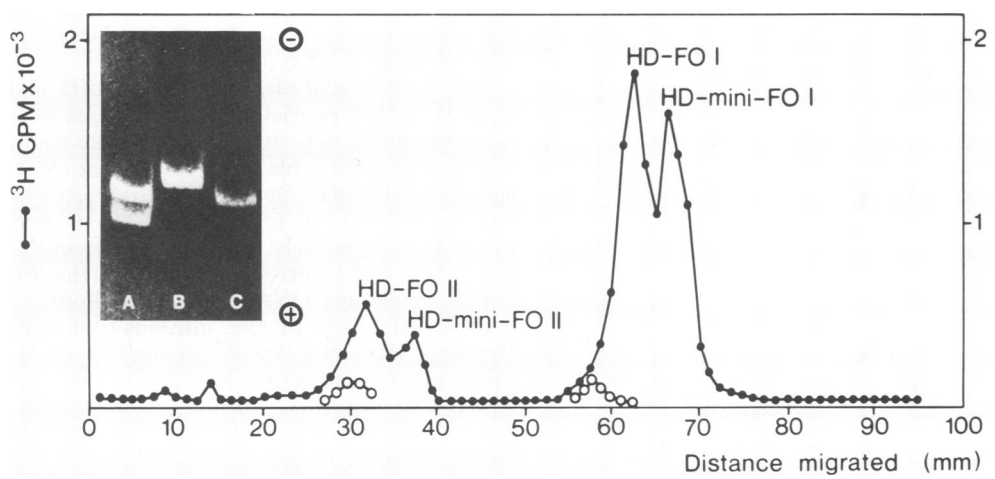

FIG. 2. *Agarose gel electrophoresis of HD DNA and HD minicircular DNA. Fractions 16 to 20 of the superhelical DNA shown in Fig. 1C were pooled and subjected to electrophoresis after removal of EtBr and desalting together with ^{32}P-labeled SV40 DNA into a 1% agarose gel. The distribution of radioactivity was determined after cutting the gel into 1-mm slices. The insert shows photographs of an agarose gel containing: (A) HD superhelical DNA isolated from Vero-76 cells cocultivated with CV-1 cells; (B) SV40 FO I DNA; and (C) HD FO I DNA from Vero-76 cells.*

ified and subjected to agarose gel electrophoresis, it could be shown that both size classes were represented within the virion particles (Fig. 4).

Analysis of both HD DNA size classes with restriction endonucleases. For comparison of their restriction enzyme cleavage patterns, HD FO I DNA was isolated from either Vero-76 clone E, which does not produce minicircular DNA (see Fig. 2, gel C), or Vero-76 cells, whereas minicircular DNA was obtained from cocultivated Vero-76–CV-1 cells. The latter DNA was separated from the larger HD DNA by electrophoresis in 1% agarose gels and elution from the gels as described (4).

Full-length linear molecules (FO III) were obtained by digestion of the superhelical DNA with S_1 nuclease. The molecular weights of both size classes of HD DNA were calculated from the electrophoretic mobilities of known SV40 reference molecules (SV40 FO III and SV40 *Hin*dIII-A fragment) in 1% agarose gels (Fig. 5). HD DNA and HD minicircular DNA are 3.45 $\times$ 10^6 daltons and, in close agreement with previously reported data (9), 3.25 $\times$ 10^6 daltons in size, respectively (Fig. 5).

The minicircular DNA has been shown to contain two endo R · *Hin*dIII cleavage sites (9). Both sites are also contained in the larger HD DNA molecules (Fig. 5). It is also shown that the *Hin*dIII-A and -B fragments are identical in size, in the case of both the larger and the minicircular molecules (1.97 $\times$ 10^6 and 1.28 $\times$ 10^6 daltons, respectively). Thus, the larger molecules must contain a further endo R · *Hin*dIII cleavage site. The resulting small fragment was revealed in a 12% polyacrylamide gel (Fig. 6),

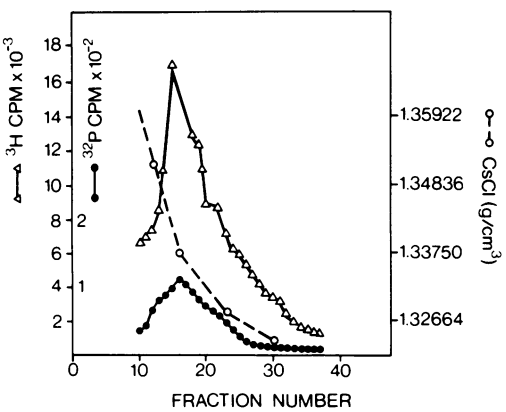

FIG. 3. *Purification of HD virions in a CsCl-density equilibrium gradient. [^{3}H]thymidine-labeled HD virus was mixed with purified ^{32}P-labeled SV40 virus and centrifuged to equilibrium as described in the text. For determination of radioactivity, 10-μl samples were measured.*

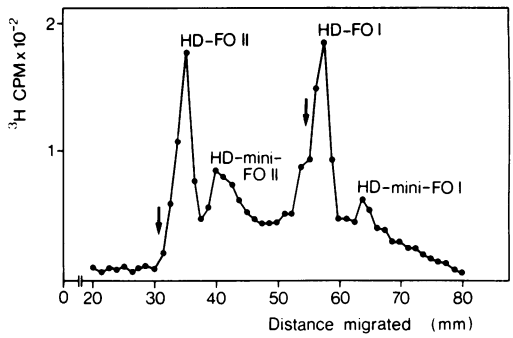

FIG. 4. *Agarose gel electrophoresis pattern of HD virion DNA. From purified HD virions (Fig. 3) the DNA was isolated by phenol extraction and a subsequent extraction with isoamylalcohol-chloroform (1:25, vol/vol) as described (8), precipitated with twice the volume of ethanol, and suspended prior to electrophoresis in 20 mM Tris–1 mM EDTA (pH 7.5). The arrows indicate the position of ^{32}P-labeled SV40 DNA.*

and its size was calculated to be 0.2 $\times$ 10^6 daltons, using fd DNA fragments with known sizes as a reference (7). The size of the HD *Hin*dIII-C fragment (0.2 $\times$ 10^6 daltons) is coincident with the difference in size between HD DNA and HD minicircular DNA (0.2 $\times$ 10^6 daltons).

As shown already, incubation of HD minicircular DNA with endo R · *Eco*RI results in two cleavage products (9). Also, the larger HD DNA is cut twice by endo R · *Eco*RI, the resulting larger *Eco*RI-A fragment being identical in size to the minicircular *Eco*RI-A fragment (1.75 $\times$ 10^6 daltons), whereas the *Eco*RI-B fragments are either 1.70 $\times$ 10^6 or 1.50 $\times$ 10^6 daltons in size, respectively (Fig. 5, gels F and G).

For further analysis, endo R · *Hin*dIII and endo R · *Eco*RI restriction endonucleases were used simultaneously to achieve double-digest products of minicircular HD DNA. Four cleavage products were obtained with molecular weights of 1.13 $\times$ 10^6, 0.93 $\times$ 10^6, 0.83 $\times$ 10^6, and 0.36 $\times$ 10^6, respectively (Fig. 7). The sum of the molecular weights corresponds well with the size of the minicircular DNA (3.25 $\times$ 10^6 daltons).

Physical maps of the minicircular and the large HD DNA. The restriction endonuclease map of minicircular HD DNA was constructed by analysis of partial endo R · *Hin*dIII-endo R · *Eco*RI cleavage products. A complete digest is shown in Fig. 7 and a partial digest, together with SV40 *Hin*dIII DNA fragments, is depicted in Fig. 8. Partial digestion was accomplished by incubating the DNA for various lengths of time with a mixture of the restriction endonucleases. Four different partial digest products were identified in the gel shown in Fig.

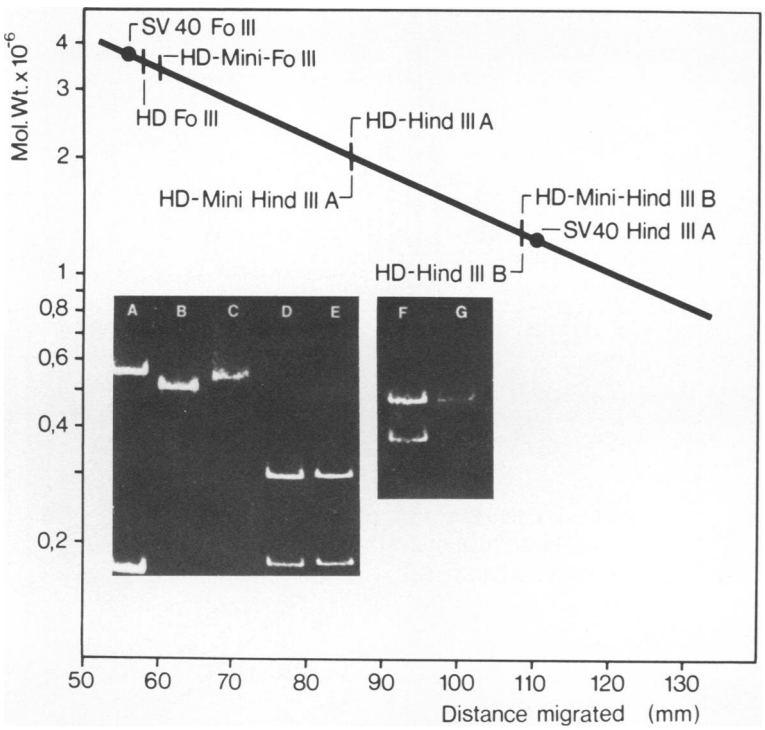

FIG. 5. *Comparison of the electrophoretic mobilities in 1% agarose and molecular weights of linear HD and SV40 DNA and of HD and SV40 DNA fragments. The photographs of the gels show SV40 DNA FO III (A, top), SV40 HindIII-A (A, bottom), HD minicircular DNA FO III (B), HD DNA FO III (C), HD minicircular DNA HindIII-A and -B (D), and HD DNA HindIII-A and -B (E). In a separate gel, HD minicircular DNA EcoRI-A and -B fragments are shown in (F) and in (G) the pattern obtained after EcoRI digestion of the larger HD DNA is displayed.*

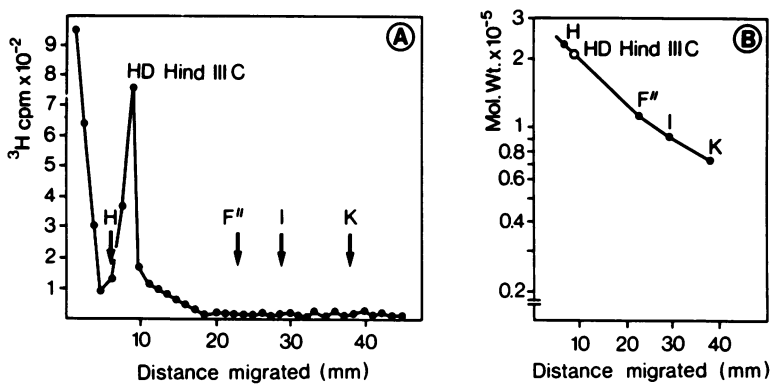

FIG. 6. *Characterization of the HD DNA fragment HindIII-C. ^{3}H-labeled HD DNA was digested with endo R · HindIII to completion and analyzed by electrophoresis in a 12% polyacrylamide gel (A) together with reference fd DNA fragments HpaI-H, -F'', -I, and -K. The positions of the fd DNA fragments are indicated by the arrows. (B) Comparison of the electrophoretic mobility of HD DNA fragment HindIII-C and the fd DNA fragments and their molecular weights.*

8. Two further partial digest fragments were obtained in a separate experiment (gel not shown). Their molecular weights and possible orders are summarized in Table 2. The data can only be reconciled with the order, *Hin*dIII-*Eco*RI-B-D-A-C.

To identify the order of the endo R · *Hin*dIII-endo R · *Eco*RI fragments within the larger HD

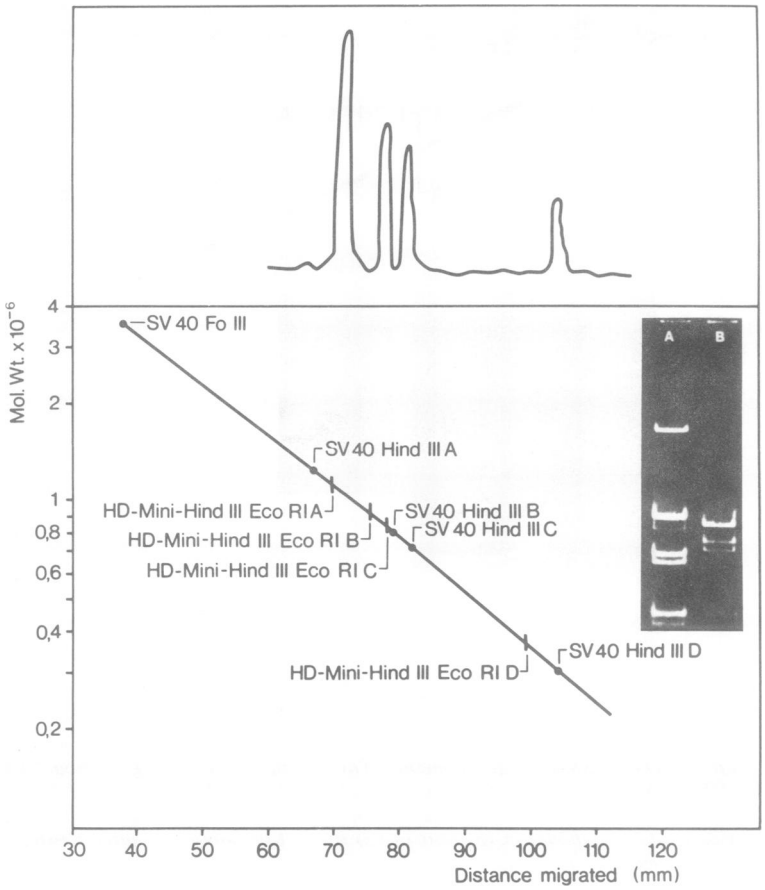

FIG. 7. *Comparison of the electrophoretic mobilities and molecular weights of double-digest products of HD minicircular DNA with SV40 DNA fragments. Minicircular HD DNA was digested simultaneously with endo R · HindIII and endo R · EcoRI restriction endonucleases under conditions that achieve complete digestion. The fragments were analyzed by electrophoresis in a 1% agarose slab gel (B). For comparison, SV40 HindIII DNA fragments were subjected to electrophoresis in a parallel track (A). A densitometer tracing of (B) is shown in the upper part of the figure.*

DNA, complete digests of both the larger and the minicircular DNA were compared with each other in the agarose gel shown in Fig. 9. As may be seen, the four fragments obtained after digestion of the minicircular DNA are also contained in the larger DNA, which, being larger by 2×10^5 daltons, contains, in addition, a fragment *Hin*dIII-*Eco*RI-E (Fig. 9D). This fragment could be shown after electrophoresis in a 12% polyacrylamide gel to be identical with the *Hin*dIII-C fragment described in Fig. 6, to which a molecular weight of 2×10^5 was assigned. Thus, the minicircular HD DNA is deleted with regard to the *Hin*dIII-C fragment.

Simultaneous incubation of minicircular DNA with the restriction endonucleases endo R · *Hin*dIII + II (Fig. 10A) generated three fragments with molecular weights of 1.97×10^6, 0.74×10^6, and 0.54×10^6, respectively. These fragments are also contained in the larger HD DNA (not shown). Simultaneous digestion of minicircular DNA with endo R · *Hin*dII + III and endo R · *Eco*RI (Fig. 10B) reveals that *Eco*RI cuts both the *Hin*dII + III-A and the small C fragments each into two smaller products. The *Hin*dII + III-B fragment remains unaffected. This notion permits the assignment of the single *Hin*dII restriction site in minicircular DNA to the *Hin*dIII-B fragment and also allows the allocation of the *Eco*RI cut within the *Hin*dIII-B fragment. The larger HD DNA contains, besides the *Hin*dII + III fragments A, B, and C (of which, as shown above, the minicircular DNA is composed), two further *Hin*dII + III fragments, D and E. These fragments are generated by a second *Hin*dII cut, which divides the frag-

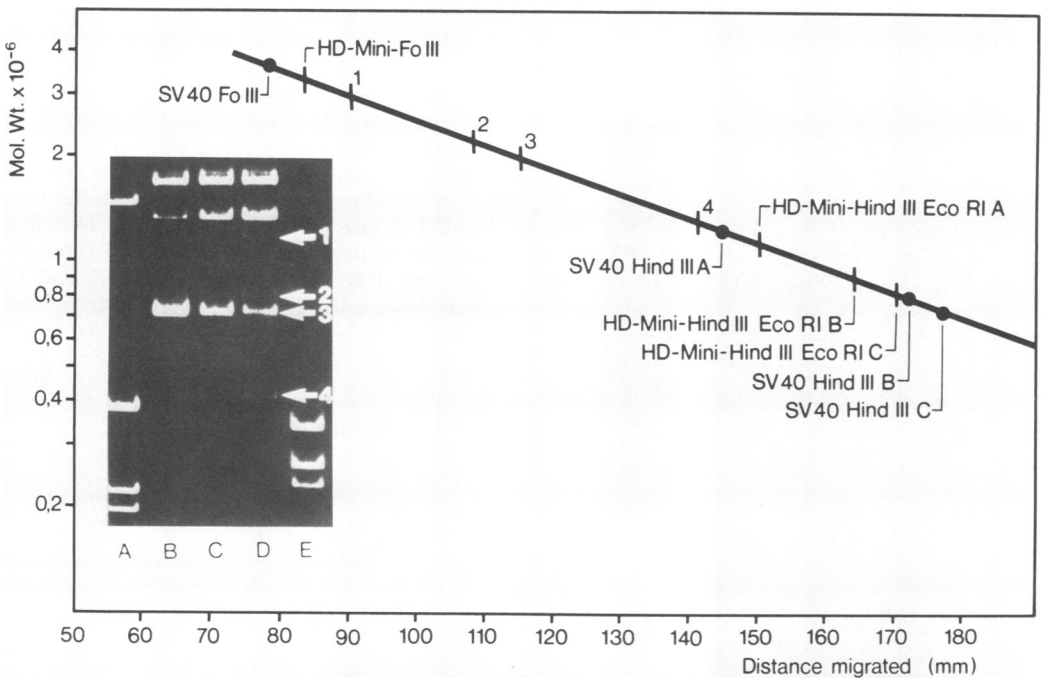

FIG. 8. *Electropherograms of partial digest fragments of HD minicircular DNA. Minicircular HD DNA was digested for various lengths of time simultaneously with endo R · HindIII and endo R · EcoRI restriction endonucleases, and the DNA fragments were analyzed by electrophoresis in a 1% agarose slab gel. For comparison, in (A) SV40 DNA FO III (top) and SV40 DNA fragments HindIII-A, -B, and -C are shown. The HD DNA was incubated with the restriction endonucleases for 1 (B), 2 (C), 6 (D) and 240 (E) min. The numbers 1 to 4 indicate the positions of partial digest products.*

ment *Hin*dIII-C into two fragments. As may be deduced from the relative electrophoretic mobilities shown in the 12% polyacrylamide gel in Fig. 11, the sum of the molecular weights of fragments *Hin*dII + III-D and -E is equal to the size of fragment *Hin*dIII-C. The location of the *Hin*dII cleavage site within fragment *Hin*dIII-C was determined using the molecular weights of partial *Hin*dII + III cleavage products. Appearance of the partial product *Hin*dII + III-A and -E (Fig. 12, arrow) showed that fragment E is adjacent to fragment A rather than to fragment C.

To ascertain the complete absence of fragments *Hin*dII + III-D and -E from minicircular DNA, 5 μg of minicircular DNA was completely digested with either endo R · *Hin*dIII or endo R · *Hin*dII + III restriction endonucleases, and the digests were subjected to electrophoresis on 12% polyacrylamide gels (Fig. 13). For comparison, equal amounts of reference *Hpa*I-digested fd DNA were also subjected to electrophoresis in the same gel. Although under these conditions fragments that are 2×10^4 daltons in size can be detected (see the smallest fd DNA *Hpa*I fragment for comparison), the complete absence of such small fragments in the case of minicircular DNA may be seen. This result confirms the data based on the molecular weights of the various restriction endonuclease fragments, a summary of which is given in Table 3. The physical map of the larger and the minicircular HD genomes in Fig. 14 is oriented such that the single endo R · *Hin*dII cleavage site in the minicircular DNA serves as the starting point at 12 o'clock.

TABLE 2. *Limit digest products obtained after incubation of minicircular HD DNA with endo R · HindIII-endo R · EcoRI*

Designation of fragment (see Fig. 8)	Mol wt of partial DNA fragments (× 10^6)	Expected sum of mol wt of limit products (×10^6)	Fragments present in partial products
None	1.75	1.76	C, B
None	1.50	1.49	A, D
1	2.87	2.89	A, C, B
2	2.30	2.32	D, A, C
3	2.10	2.12	C, B, D
4	1.28	1.29	B, D

The above conclusions on the structural relationship between minicircular and large HD DNA were substantiated by blot hybridization

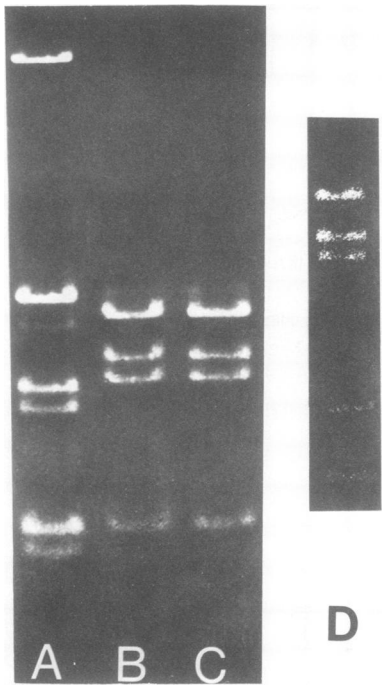

FIG. 9. *Comparison of double-digest products derived from HD DNA and HD minicircular DNA. HD DNA and HD minicircular DNA were digested simultaneously with endo R · HindIII and endo R · EcoRI restriction endonucleases under conditions that achieve complete digestion. The fragments were analyzed by electrophoresis in a 1% agarose gel. (A) SV40 DNA FO III and SV40 DNA fragments HindIII-A, -B, -C, -D, -E; (B) minicircular HD DNA; (C) HD DNA. The smallest fragment, HindIII-EcoRI-E, is not shown in (C) but is revealed in the separate 1.7% agarose gel in (D).*

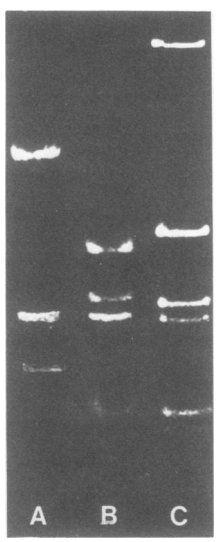

FIG. 10. *Electropherogram of HD minicircular DNA double-digest products in a 1% agarose slab gel. (A) Minicircular HD DNA digested simultaneously with endo R · HindII + III restriction endonucleases. (B) Minicircular HD DNA digested simultaneously with restriction endonucleases endo R · HindII + III and endo R · EcoRI. The smallest resulting product in (B) is not shown here. (C) SV40 DNA FO III and SV40 DNA HindIII-A, -B, -C, -D, -E.*

experiments, which also showed that the minicircular DNA sequences are represented in the large HD DNA. Minicircular ^{32}P-labeled DNA was used for hybridization with the *Hin*dIII fragments of HD DNA (Fig. 15B and C). As expected, minicircular DNA sequences are homologous to the HD DNA fragments *Hin*dIII-A and -B, whereas they are missing in fragment *Hin*dIII-C (see arrows). There is no homology between minicircular HD DNA and repetitive Vero cell DNA sequences (Fig. 15A and C), where Vero cell DNA was subjected to hybridi-

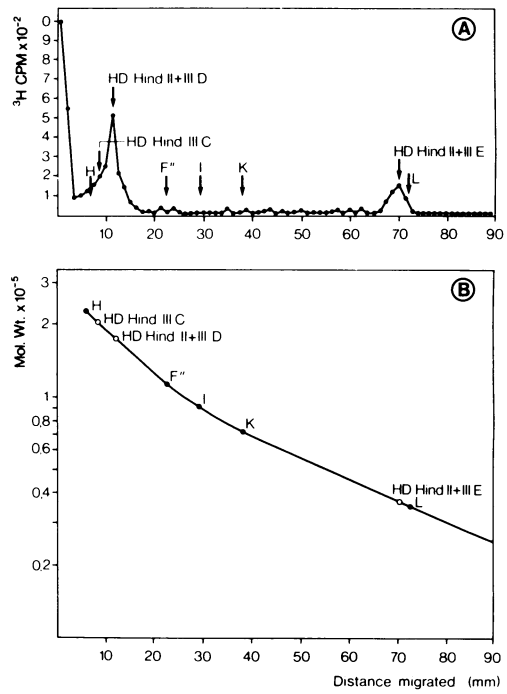

FIG. 11. *Characterization of the HD DNA fragments HindII + III-D and -E. (A) ^{3}H-labeled HD DNA was digested with endo R · HindII + III to completion and analyzed by electrophoresis in a 12% polyacrylamide gel together with reference fd DNA fragments HpaI-H, -F'', -J, -K, and -L. The position of HD DNA fragment HindIII-C (see also Fig. 6) as determined in a parallel track of the same gel is indicated by the arrow at 9 mm. (B) Comparison of the electrophoretic mobility of HD DNA fragments HindII + III-D and -E and the fd DNA fragments and their molecular weights.*

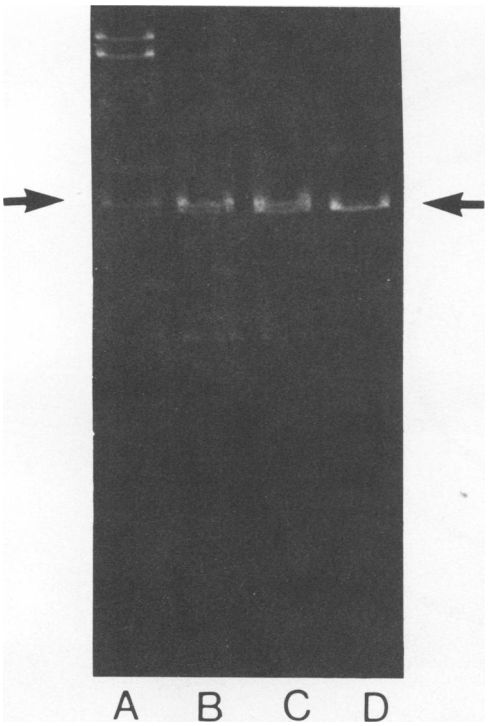

FIG. 12. *Electropherograms of partial digest fragments of HD DNA. HD DNA was digested for various lengths of time with endo R · HindII + III restriction endonuclease, and the DNA fragments were analyzed by electrophoresis in a 1% agarose slab gel. The HD DNA was incubated with the restriction endonucleases for 5 (A), 10 (B), 15 (C), and 120 (D) min. The arrows indicate the position of the partial digest product HindII + III-A + E.*

zation conditions alone or mixed with HD *Hin*dIII DNA fragments. Due to the small amount of Vero DNA assayed (0.5 μg/track) and the short time of exposure of the X-ray film to the filter, integrated HD DNA sequences would not become apparent within the Vero cell DNA. In Fig. 15D–F, nick-translated ^{32}P-labeled Vero cell DNA was used for hybridization with homologous unlabeled Vero cell DNA alone and mixed with HD *Hin*dIII DNA fragments. Again, under the experimental conditions chosen here there is no homology revealed between repetitive cellular and HD DNA.

DISCUSSION

In this work we have shown that there exist two distinctly different size classes of superhelical HD DNA. Both can be encapsidated into virion particles. The order of various restriction endonuclease cleavage products was determined, and physical maps of both classes of DNA molecules were constructed. The minicircular class of HD DNA is approximately 6% smaller than the large size class and has arisen as a result of a deletion, since size and arrangement of all but the deleted DNA fragments are identical.

The deletion comprises, apparently as the result of a coincidence, the fragment *Hin*dIII-C, which maps between positions 0.15 and 0.21. It seems peculiar that the minicircular DNA is deleted with regard to the two endo R · *Hin*dIII restriction endonuclease recognition sites flanking fragment *Hin*dIII-C; it should, however, be pointed out that the size of fragments as large as *Hin*dIII-A (1.97×10^6 daltons) and -B (1.28×10^6 daltons) can be determined in 1% agarose only within a range of error of $\pm 2 \times 10^4$ daltons. Thus, the conclusion that minicircular DNA

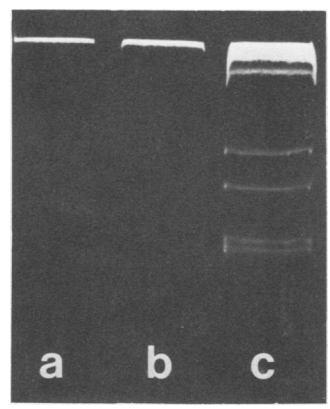

FIG. 13. *Absence of fragments HindII + III-D and -E from HD minicircular DNA. HD minicircular DNA (5 μg) was incubated under conditions that achieve complete digestion with either endo R · HindII + III (a) or endo R · HindIII (b) and applied to a 12% polyacrylamide gel. For comparison, fd DNA HpaI fragments were subjected to electrophoresis in the same gel (c). The lowermost fragment in (c) represents fd DNA fragment K (for comparison, see Fig. 11).*

TABLE 3. *Molecular weights of restriction endonuclease fragments of HD and HD minicircular DNA*

Fragment	Mol wt		
	HD minicircular DNA	HD DNA (%)	
*Hin*dII + III-A	1.97×10^6	1.97×10^6	(57)
*Hin*dII + III-B	0.74×10^6	0.74×10^6	(21)
*Hin*dII + III-C	0.54×10^6	0.54×10^6	(16)
*Hin*dII + III-D		0.16×10^6	(5)
*Hin*dII + III-E		0.036×10^6	(1)
*Eco*RI-A	1.75×10^6	1.75×10^6	(51)
*Eco*RI-B	1.50×10^6	1.70×10^6	(49)
FO III	3.25×10^6	3.45×10^6	(100)

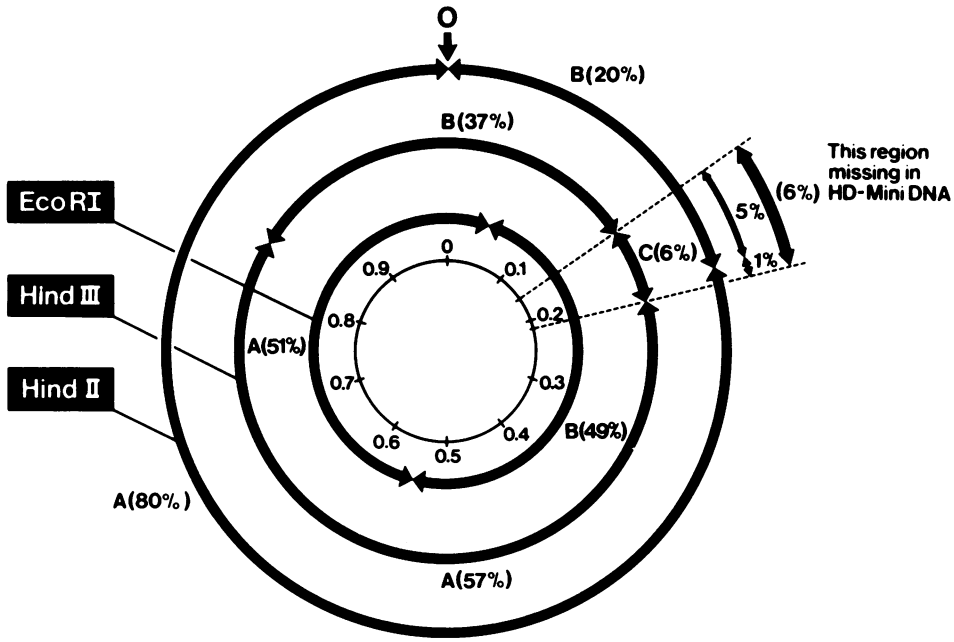

FIG. 14. *Physical map of the HD genome (molecular weight, 3.45 × 10⁶).*

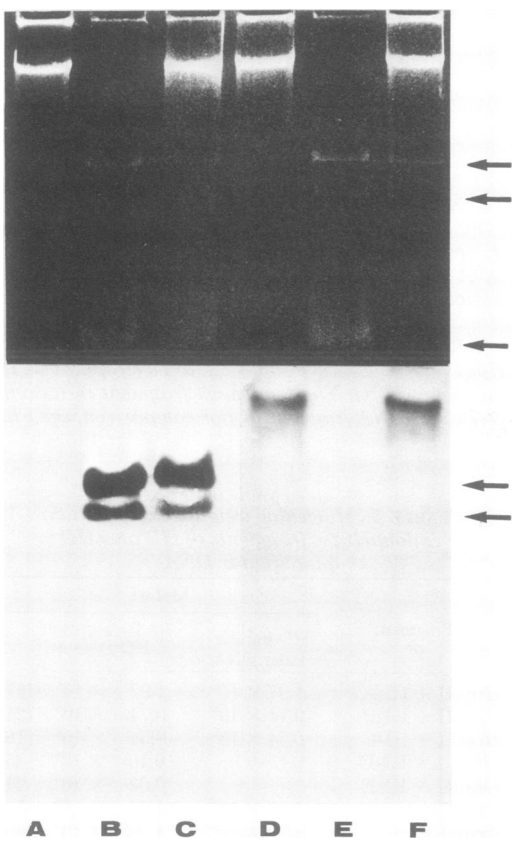

happens to miss precisely the *Hin*dIII-C fragment is less compelling.

The availability of a naturally occurring deleted DNA molecule raises the possibility of assaying minicircular HD DNA by transfection of RITA cells for its biological activity. Experiments along these lines are under way. The availability of only small amounts of purified minicircular DNA together with the low effi-

FIG. 15. *Electropherograms of HD DNA HindIII fragments and Vero DNA and hybridization with either ^{32}P-labeled minicircular or ^{32}P-labeled Vero DNA. HD DNA was cleaved with endo R · HindIII restriction endonuclease and subjected to electrophoresis either separately (0.1 μg/track) or after mixing with uncleaved Vero DNA (0.5 μg/track) into a 1% agarose slab gel. The Vero DNA was isolated from cells which were proven to lack presence of HD DNA-FO I (9). After electrophoresis the slab gel was stained with EtBr and photographed under UV to mark the positions of the respective DNA probes (upper). Then the DNA was denatured within the gel and transferred on nitrocellulose filters. DNA-DNA hybridization was carried out using either minicircular DNA (A–C) or Vero DNA (9) (D–F), which were both labeled by nick translation (specific activity, 10^8 cpm/μg of DNA). An autoradiograph (lower) was made by exposing X-ray films to the filters overnight. The arrows indicate the positions of HindIII fragments A, B, and C. (A) Vero DNA; (B) HD HindIII fragments; (C) Vero DNA + HD HindIII fragments; (D) Vero DNA; (E) HD HindIII fragments; (F) Vero DNA + HD HindIII fragments.*

ciency of RITA cells regarding HD DNA replication have hampered the progress of these experiments. However, the notion that all of the clonal lines that were derived from the HD virus-producing Vero-76 cell culture produced exclusively the larger type of HD DNA suggests that the deletion within the minicircular DNA may comprise a region of the viral genome that is indispensable for vegetative growth of the virus. It is conceivable that replication of minicircular HD DNA may depend on the presence of complementing larger HD DNA.

As yet, the origin of HD virus is unclear. The results of the blot hybridization experiment (Fig. 15), although apparently not revealing the presence of multiple copies of HD DNA per Vero cell genome, do not preclude, as mentioned already, the presence of small amounts of integrated or episomal HD DNA sequences. Therefore, the possibility exists that HD virus persisted in our Vero cells in either an integrated or a free state ever since they had been established as a cell line. It is also possible, although less likely, that HD virus arose in another species and was somehow transferred to our strain of Vero cells. An answer will be provided with the help of blot experiments, in which the DNA of Vero cells of various sources will be examined for the presence of integrated HD DNA sequences (manuscript in preparation). If it is demonstrated that HD DNA sequences are present in all Vero cells in an integrated state, our Vero-76 cells, which as shown in this study produce temporarily free HD superhelical DNA (and virus), will provide an interesting system for the investigation of activation of integrated viral DNA sequences.

ACKNOWLEDGMENTS

We thank E. Sauer, V. Geis, M. Pernfuss, W. Baader, and P. Naber for technical assistance. P. Gruss kindly provided the nick-translated DNA and was of help with the blotting technique.

This work was supported by a grant from the Bundesminister für Forschung und Technologie.

LITERATURE CITED

1. **Botchan, M., W. Topp, and J. Sambrook.** 1976. The arrangement of simian virus 40 sequences in the DNA of transformed cells. Cell **9**:269–287.
2. **Gruss, P., and G. Sauer.** 1975. Repetitive primate DNA containing the recognition sequences for two restriction endonucleases which generate cohesive ends. FEBS Lett. **60**:85–88.
3. **Gruss, P., and G. Sauer.** 1977. Infectious linear DNA sequences replicating in simian virus 40-infected cells. J. Virol. **21**:565–578.
4. **Jensen, F. C., A. J. Girardi, R. V. Gilden, and H. Koprowski.** 1964. Infection of human and simian tissue cultures with Rous sarcoma virus. Proc. Natl. Acad. Sci. U.S.A. **52**:58–59.
5. **Ketner, G., and T. J. Kelly.** 1976. Integrated simian virus 40 sequences in transformed cell DNA: analysis using restriction endonucleases. Proc. Natl. Acad. Sci. U.S.A. **73**:1102–1106.
6. **Macpherson, I., and L. Montagnier.** 1964. Agar suspension culture for the selective assay of cells transformed by polyoma virus. Virology **23**:291–294.
7. **Seeburg, H. P., and H. Schaller.** 1975. Mapping and characterization of promotors in bacteriophages fd, f1 and M13. J. Mol. Biol. **92**:261–277.
8. **Waldeck, W., K. Chowdhury, P. Gruss, and G. Sauer.** 1976. Random cleavage of superhelical SV40 DNA by S_1 nuclease. Biochim. Biophys. Acta **425**:157–167.
9. **Waldeck, W., and G. Sauer.** 1977. New oncogenic papovavirus from primate cells. Nature (London) **269**:171–173.
10. **Yasumura, T., and T. Kawakita.** 1963. Nippon Rinsho **21**:1201.